The L cell transcriptome is unaffected by vertical sleeve gastrectomy but highly dependent upon position within the gastrointestinal tract

Rollins, Katherine A ; Opitz, Lennart ; Arnold, Myrtha ; Simon, Eric ; Neubauer, Heike ; Wolfrum, Susanne

Abstract: Altered GLP-1 secretion from L cells has been implicated in the development of type 2 diabetes mellitus and its resolution following bariatric surgery. However, changes in L cell gene expression, which may form the basis for altered functionality after high fat diet (HFD) or bariatric surgery, have either not been investigated or have given conflicting results. We developed a gcg-DTR-eGFP reporter mouse to isolate ileal and colonic L cells from HFD fed insulin resistant mice and mice showing improved glucose tolerance following vertical sleeve gastrectomy (VSG). Transcriptomic sequencing and identification of genes differentially expressed in response to HFD or VSG revealed small changes with HFD, primarily in immune related genes, but no regulation following VSG. In contrast, large differences were observed between ileal and colonic L cells due to the differential expression of genes involved in nutrient transport and metabolism, reflecting to some extent the differences in the surrounding epithelium. We showed that, in line with the gene expression data, colonic and ileal L cells exhibit differing GLP-1 responses to nutrients (glucose and the gly-sar dipeptide) and hormones (vasopressin). Thus, we hypothesise that colonic and ileal L cells have different physiological roles, with ileal L cells contributing more to postprandial glucose homeostasis by responding to dietary nutrients and colonic cells responding more to non-dietary stimulants.

DOI: https://doi.org/10.1016/j.peptides.2019.01.001

Peptides 113 (2019) 22–34

Contents lists available at ScienceDirect

Peptides

journal homepage: www.elsevier.com/locate/peptides

The L cell transcriptome is unaffected by vertical sleeve gastrectomy but highly dependent upon position within the gastrointestinal tract

Katherine A. Rollins[a], Lennart Opitz[b], Myrtha Arnold[c], Eric Simon[d], Heike Neubauer[e], Susanne Wolfrum[a,*]

[a] Laboratory of Organic Chemistry, ETH Zurich, Schorenstrasse 16, 8603, Schwerzenbach, Switzerland
[b] Functional Genomics Center Zurich, University of Zurich/ETH Zurich, Winterthurerstrasse 190, 8057, Zürich, Switzerland
[c] Physiology and Behavior Laboratory, ETH Zurich, Schorenstrasse 16, 8603 Schwerzenbach, Switzerland
[d] Boehringer Ingelheim Pharma GmbH & Co KG, Target Discovery Research Department, Birkendorfer Strasse 65, 88397, Biberach/Riss, Germany
[e] Boehringer Ingelheim Pharma GmbH & Co KG, Cardiometabolic Diseases Research Department, Birkendorfer Strasse 65, 88397, Biberach/Riss, Germany

ARTICLE INFO

Keywords:
GLP-1
Enteroendocrine L cells
RNA sequencing
High fat diet
Vertical sleeve gastrectomy

ABSTRACT

Altered GLP-1 secretion from L cells has been implicated in the development of type 2 diabetes mellitus and its resolution following bariatric surgery. However, changes in L cell gene expression, which may form the basis for altered functionality after high fat diet (HFD) or bariatric surgery, have either not been investigated or have given conflicting results. We developed a *gcg*-DTR-eGFP reporter mouse to isolate ileal and colonic L cells from HFD fed insulin resistant mice and mice showing improved glucose tolerance following vertical sleeve gastrectomy (VSG). Transcriptomic sequencing and identification of genes differentially expressed in response to HFD or VSG revealed small changes with HFD, primarily in immune related genes, but no regulation following VSG. In contrast, large differences were observed between ileal and colonic L cells due to the differential expression of genes involved in nutrient transport and metabolism, reflecting to some extent the differences in the surrounding epithelium. We showed that, in line with the gene expression data, colonic and ileal L cells exhibit differing GLP-1 responses to nutrients (glucose and the gly-sar dipeptide) and hormones (vasopressin). Thus, we hypothesise that colonic and ileal L cells have different physiological roles, with ileal L cells contributing more to postprandial glucose homeostasis by responding to dietary nutrients and colonic cells responding more to non-dietary stimulants.

1. Introduction

Enteroendocrine L cells are classically defined as secreting glucagon-like peptide-1 (GLP-1) and peptide tyrosine tyrosine (PYY), and are enriched in the distal regions of the gastrointestinal (GI) tract [1]. GLP-1 plays an important role in postprandial glucose homeostasis as it acts as an incretin hormone, promoting pancreatic glucose-dependent insulin secretion, while also inhibiting gastric emptying and suppressing appetite [2]. Recently, it has been shown that L cells co-express several additional hormones and that upper small intestine (SI) L cells are more similar to upper SI K cells, which classically express gastric inhibitory peptide (GIP), than colonic L cells [3].

Postprandial GLP-1 secretion has been reported to be blunted in obese and diabetic patients [4–6], which may contribute to the development of type 2 diabetes mellitus (T2DM) [7], although this is not consistently observed [8]. Currently it is unclear how the murine L cell responds to high fat diet (HFD) and peripheral insulin resistance as L cell density and marker gene expression have been reported to be both increased [9,10] and decreased [11,12] after 2–16 weeks HFD. Bariatric surgical techniques, including vertical sleeve gastrectomy (VSG), are the most efficacious treatment method for obesity and T2DM [13], resulting in early improvements in metabolic parameters before weight loss occurs [14]. These improvements are consistently associated with increased postprandial circulating GLP-1 [15–17], resulting from increased nutrient delivery to the distal gut. In addition, L cell density may be increased [18] or unchanged [19] after VSG, and the nutrient

Abbreviations: HB-EGF, heparin-binding epidermal growth factor; DTR, diphtheria toxin receptor; VSG, vertical sleeve gastrectomy; GO, gene ontology; MDS, multidimensional scaling; DE, differentially expressed

* Corresponding author.
E-mail addresses: katherine.rollins@org.chem.ethz.ch (K.A. Rollins), lennart.opitz@fgcz.ethz.ch (L. Opitz), myrtha-arnold@ethz.ch (M. Arnold), eric.simon@boehringer-ingelheim.com (E. Simon), heike.neubauer@boehringer-ingelheim.com (H. Neubauer), wolfrum@org.chem.ethz.ch (S. Wolfrum).

https://doi.org/10.1016/j.peptides.2019.01.001
Received 27 September 2018; Received in revised form 7 December 2018; Accepted 9 January 2019
Available online 17 January 2019

sensitivity of the L cell may be affected [20]. However, the contribution of elevated postprandial GLP-1 to the improved metabolic phenotype is debated [21–23]. GLP-1 mimetics have been recently introduced to the clinic for the control of blood glucose in T2DM, as the incretin effect is preserved in T2DM patients, and for the treatment of obesity [24]. Targeting GLP-1 responses remains a viable treatment approach for diabetic patients, but to date our understanding of L cells is limited, especially the mechanisms underlying the changes seen during insulin resistance and following bariatric surgery.

Here, we transcriptionally characterise ileal and colonic L cells and epithelial cells to examine their role in the development of metabolic disease and its resolution following bariatric surgery. Transcriptomic characterisation following HFD and VSG was used to investigate the mechanisms underlying changes in GLP-1 secretion under these conditions and to determine if other L cell properties are also altered and contribute to the metabolic phenotype. In addition, we examine the differences in L cells between tissues, how the differences in L cells reflect changes in the surrounding epithelium and the consequence of these differences on the current paradigm of L cell function.

2. Experimental procedures

2.1. Materials

All chemicals were purchased from Sigma-Aldrich unless otherwise specified.

2.2. Animals

2.2.1. gcg-DTR-eGFP mice

The new mouse strain *gcg*-DTR-eGFP was prepared using Red / ET recombination technology (Gene Bridges) as described previously [25]. Briefly, a cassette containing a primate heparin-binding epidermal growth factor-like growth factor (HB-EGF, here diphtheria toxin receptor, DTR) / enhanced green fluorescent protein (eGFP) fusion gene and a polyA sequence combined with a neo / kana resistance cassette flanked by frt sites was amplified by PCR with primers providing overhangs for a direct recombination into the *gcg* (*Preproglucagon*) coding region of the murine *gcg* locus of the bacterial artificial chromosome (BAC) RP23-343 C17 (BACPAC Resources Center) which contains the mouse *gcg* genomic sequence. Importantly, all upstream and downstream regulatory sequences were included in the construct. The experimental procedures for preparation and purification of the final BAC are described in detail by Johansson et al. [26]. Cloning primers are listed in Supplementary Information Table 1 and schematic representations of the constructs are depicted in Fig. 1A. Transgenic mice were generated by pronuclear injection into C57BL/6 N oocytes according to standard procedures [27]. Transgene copy number was estimated to be one by comparing C_t values for a transgene specific probe vs. a probe recognizing apolipoprotein B (*apoB*).

2.2.2. Animal procedures

All animal work was approved by the cantonal veterinary office of Zurich. Mice were kept in grouped cages on a 12 / 12 h light/dark cycle in a pathogen-free animal facility with *ad libitum* access to food and water. Mice were kept on standard laboratory chow (#3436, Kliba Nafag, composition: https://www.serlab.com/uploads/1/1/0/3/110311153/3436_souris_et_ratentretien_extrudat.pdf) or placed on a purified high fat diet (HFD) consisting of 60% calories from fat (#2127, Kliba Nafag, composition: http://www.kliba-nafag.ch/neutral/download/2127.pdf). For the tolerance tests, mice were fasted for 6 h prior to either *i.p.* injection of 0.6 U/kg insulin (Actrapid, Novo Nordisk) for the insulin tolerance test or intragastric gavage of 200 µl Ensure Plus liquid diet (29.5% calories from fat, 53.8% from carbohydrate and 16.7% from protein) for the mixed meal tolerance test. Blood glucose was measured from the tail vein using an Accu-Check Aviva blood glucose monitor (Roche). Awake mice were scanned using the EchoMRI 3-in-1 analyzer (EchoMRI™, Singapore and Houston) to assess fat and lean mass. For determination of plasma GLP-1, mice were fasted for 4 h prior to gavage of 2.4 g glucose/kg body weight. Blood was collected from the tail vein 4 min after gavage into tubes with EDTA and DPP-IV inhibitor (Millipore) and plasma separated by centrifugation. GLP-1 concentrations were measured using the active GLP-1 v.2 kit (Meso Scale Discovery, sensitivity 0.12 pg/ml, 31% cross-reactivity to GLP-1 (7–37) and 0.1% to GLP-1 (9–36) amide). All experiments were performed with male mice, HFD was begun around 8 weeks of age.

2.2.3. VSG and sham surgery

For the surgery, mice were housed 2–3 per cage and had been on HFD for 19–22 weeks. 4 days prior to surgery, mice were offered a highly viscous semi-solid porridge meal made of oat flakes cooked with water for 2 h to expose the mice to the unfamiliar taste and texture. The last 3 days prior to surgery, mice had the choice between HFD and chow and 2 h prior to surgery food was withdrawn. A broad-spectrum antibiotic enrofloxacin (10 mg/kg, Baytril 2.5%, Bayer) and the analgesic caprofen (5 mg/kg, Norocarp, UFAMED) were administered subcutaneously 2 and 1 h(s) prior to surgery, respectively. All surgeries were performed under aseptic conditions. After induction of anaesthesia with isoflurane (Isoflo, Zoetis Schweiz GmbH), an upper midline laparotomy was performed over a length of 1.5 cm to the xiphoid cartilage and a self-retaining retractor was placed. The liver was gently retracted and the stomach freed by cutting the perigastric ligaments, and all branches of the gastroepiploic vessels were carefully ligated and cut close to the greater curvature of the stomach. For the vertical sleeve gastrectomy (VSG), a tubular sleeve was created by applying a titanium clip (LIGACLIP, Johnson and Johnson) on the stomach from 3 mm proximal to the pylorus, to the gastroesophageal junction (Angle of His) always leaving the same stomach volume. The greater curvature was dissected along the clip aiming for a resection of over 75% of gastric volume including the complete fundus. 4–6 single stitches with 8-0 polyamid suture (Johnson and Johnson) were applied around the clip for additional fixation. After relocating the gastric sleeve, the laparotomy was closed by continuous muscle and skin suture (6-0 Vicryl, Johnson and Johnson). The procedure for the sham surgery was similar to VSG except a small titanium clip (B9180, Vitalitec) was applied at the greater curvature, leading to a restriction of less than 10% of gastric volume. After the surgical procedure, animals promptly emerged from anaesthesia and were returned to their home cage, which was placed on a heating pad for the first night. Mice were offered porridge for around 24 h and switched back to HFD thereafter. Antibiotics were given for one and analgesics for 3 postoperative days.

2.3. Immunofluorescence

9 µm cryo-sections were fixed with 4% paraformaldehyde and permeablised with triton X-100, before blocking with donkey serum. Sections were incubated overnight with primary antibodies targeting GFP (ab5450, Abcam) and GLP-1 (sc-7782, Santa Cruz), before incubation with fluorophore tagged secondary antibodies. Control sections were stained with secondary antisera alone.

2.4. Purification of L cells by FACS and RNA extraction

For FACS purification of L cells, mice were sacrificed with CO_2 and the colon and ileum (the distal half of the SI) were washed in PBS on ice. Gut pieces were cut open longitudinally and incubated in successive tubes of PBS with 1.5 mM EDTA and 0.5 mM DTT with rocking at 37 ^{0}C, and cells were released by agitation at the end of each incubation. The first fraction was disposed of, and the remainder stored as a pellet on ice before combining and washing in PBS. Single cell suspensions were sorted by flow cytometry using side scatter, forward scatter, pulse

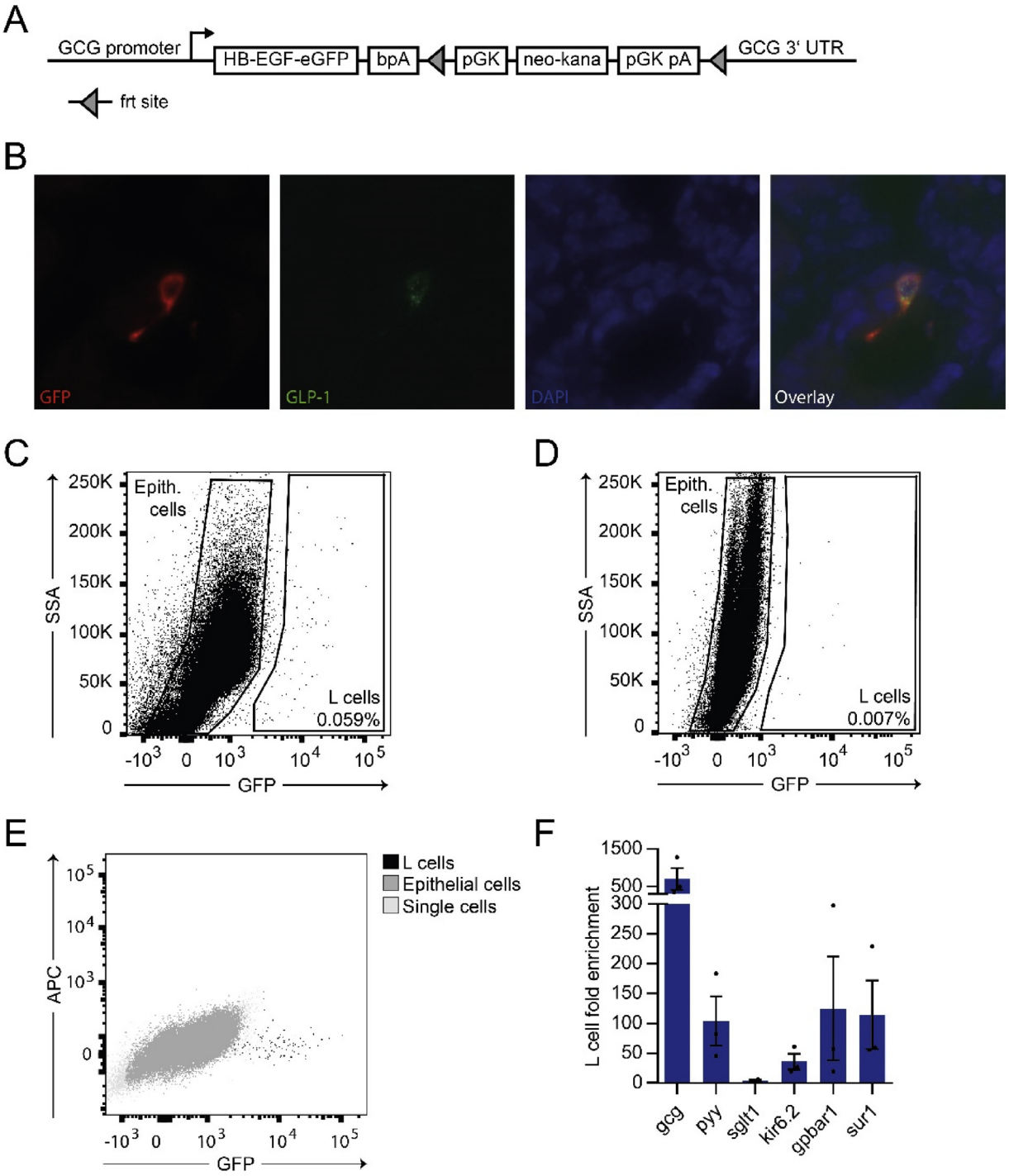

Fig. 1. Generation and validation of the *gcg*-DTR-eGFP reporter mouse and L cell purification. (A) Schematic representation of the targeting construct used to generate the *gcg*-DTR-eGFP mouse strain. (B) Co-localisation of GFP and GLP-1 by immunofluorescence in the ileum (23 week chow diet mouse). Representative plots of the gates used to sort colonic (C) and ileal (D) L cells and epithelial cells from all live single cells based on GFP intensity. Previously, dead cells were excluded based on high DAPI intensity and aggregates and debris excluded based on side scatter and forward scatter. (E) GFP vs. APC (empty channel) plot of sorted colonic epithelial and L cells. (F) Quantification of known L cell enriched genes by qPCR in sorted colonic L cells, mean ± SEM shown, n = 3.

width and DAPI intensity gates to exclude debris, aggregates and dead cells, then L cells and epithelial cells were selected based on GFP (FITC) intensity. Cells were sorted directly into lysis buffer and total RNA was isolated using the RNeasy Plus Micro kit (Qiagen).

2.5. Quantitative RT-PCR

cDNA was synthesised using the high-capacity cDNA reverse transcription kit (Applied Biosystems) and used for RT-qPCR reactions using FAST SYBR green. Target gene expression was compared to that of *gapdh* and *36B4* from the same sample and then L cells compared to epithelial cells from the same mouse using the $2^{-\Delta\Delta Ct}$ method.

2.6. Transcriptome sequencing

10 ng of total RNA was converted to cDNA using the Ovation RNA-

Seq System V2 (NuGEN Technologies), which provides coverage of non-coding (ncRNAs) and non-polyadenylated RNA transcripts in addition to protein-coding mRNAs, while reducing ribosomal RNA conversion to cDNA. Libraries were generated according to recommended procedures, using the Illumina TruSeq methods. Sequencing was carried out using the Illumina HiSeq 2000 system according to Illumina protocols as 85 bp, single reads and 7 bases index read. The raw reads were first cleaned by removing reads with low quality (phred quality < 20) using Trimmomatic [28]. Sequence alignment of the resulting high-quality reads to the Mus musculus reference genome (build GRCm38.p5) and quantification of gene level expression (Ensembl release 89) was carried out using RSEM (Version 1.3.0) [29]. One colonic chow sample was excluded from further analysis due to having < 5 million reads mapping to exonic regions. A high proportion of rRNA reads were observed in all samples due to the methods used (typically 40–60%), but the large number of reads per sample ensured a sufficient depth of sequencing.

To detect differentially expressed genes we applied the count based negative binomial model implemented in the software package EdgeR (R version: 3.4.0, EdgeR version: 3.18.1) [30]. Multiple testing correction to calculate the false discovery rate (fdr) was performed using the Benjamini and Hochberg method. Heatmaps and sample clustering are based on EdgeR normalized values (TMM method). No batch effect was seen when comparing samples from the two experiments and sequencing runs (HFD / chow and VSG / sham). Sequence data that support this study have been deposited in European Nucleotide Archive (ENA) with the primary accession code PRJEB23754.

2.7. Sequencing data analysis

Differentially expressed genes were defined as expressed genes, those with a normalized count > 20 in at least half of the samples in at least one of the conditions in the comparison, with an absolute log2 ratio > 1 and an fdr of less than 5%. Gene ontology (GO) enrichment analysis (terms defined by the GO Consortium, http://www.geneontology.org/) was performed using GOrilla (Gene Ontology enRIchment anaLysis and visuaLizAtion tool) [31,32], comparing an unranked list of differentially expressed genes against a background of genes expressed in the relevant comparisons. KEGG (Kyoto Encyclopaedia of Genes and Genomes) pathway enrichment analysis was performed using DAVID 6.8 [33,34], again by comparing an unranked list of differentially expressed genes against a background of expressed genes (pathway names defined in the KEGG pathway database, https://www.genome.jp/kegg/pathway.html).

2.8. Nutrient stimulation of primary mixed cultures

Mixed primary cultures were prepared from the colon and distal most 12 cm of the SI as published [35]. Briefly, tissues were harvested and washed in L-15 on ice, the muscle layer removed by dissection, and the remaining mucosa and submucosa were digested in successive incubations of collagenase XI. Harvested crypts were plated on matrigel coated 24 well plates and left to recover overnight. Cells were washed and stimulated for 2 h in a salt bath solution (138 mM NaCl, 4.5 mM KCl, 4.2 mM $NaHCO_3$, 1.2 mM Na_2HPO_4, 2.5 mM $CaCl_2$, 1.2 mM $MgCl_2$, 10 mM Hepes pH 7.4, 0.1% fatty acid free BSA). Test compounds (glucose, arginine-vasopressin acetate or glycyl-sarcosine) and DPP-IV inhibitor (Millipore) were added for the stimulation. The supernatant was harvested, floating cells removed by pelleting, and the cultured cells lysed (50 mM Tris pH 7.4, 150 mM NaCl, 1% IGEPAL-CA 630, 0.5% deoxycholic acid, protease and DPP-IV inhibitors). Samples were stored at -80 ^{0}C before active GLP-1 concentrations were measured with the active GLP-1 v.2 kit (Meso Scale Discovery, sensitivity 0.12 pg/ml, 31% cross-reactivity to GLP-1 (7–37) and 0.1% to GLP-1 (9–36) amide).

2.9. Statistics

Data was analysed and statistical analyses performed using Graph Pad Prism 7.0.3 and R x64 3.4.2, applying *t*-tests with Welch's correction for non-equal variances and correcting for multiple testing using Bonferroni correction where relevant. Results are presented as mean ± SEM (standard error of the mean). A p-value < 0.05 was considered significant.

3. Results

3.1. The gcg-DTR-eGFP reporter mouse can be used to isolate a population of gcg-expressing (L) cells

We generated the *gcg*-DTR-eGFP mouse in which all L cells, here defined as *gcg*-expressing cells, are fluorescently labelled (the construct used is depicted in Fig. 1A). The specificity of GFP expression within the intestine was confirmed by immunofluorescence which showed co-staining of GFP and GLP-1 in cells with typical L cell morphology (Fig. 1B). The co-expression of DTR enables the specific ablation of these cells using diphtheria toxin, which is the subject of further studies not included here.

The *gcg*-DTR-eGFP reporter mouse was used to isolate L cells and the surrounding epithelial cells by FACS. Cells isolated from the ileum and colon were gated for live cells using DAPI, debris and aggregates were excluded based on side scatter and forward scatter, and finally epithelial and L cells were selected based on GFP intensity using a wild type control to determine the gating (Fig. 1C and D). GFP signal specificity was confirmed by the absence of high autofluorescence in the empty APC channel (Fig. 1E). As expected, only a low proportion of total cells were GFP positive, with a higher proportion observed in the colon than the ileum. L cells are classically defined as secreting GLP-1 and PYY, encoded by *gcg* and *pyy* respectively whose expression was strongly enriched in purified L cells compared to epithelial cells, 700-fold for *gcg*, confirming the sorting specificity (Fig. 1F). Similarly, the K_{ATP}-channel subunit genes *kir6.2* and *sur1*, the sodium-coupled glucose transporter *sglt1*, and the bile acid receptor *gpbar1* (TGR5), which have all previously been shown to be L cell enriched [36], were also enriched here (Fig. 1F).

3.2. Global sequencing analysis confirms overlap of enteroendocrine hormone expression, and shows large differences between tissues

To determine the effect of high fat diet (HFD) and vertical sleeve gastrectomy (VSG) on the L cell transcriptome, male *gcg*-DTR-eGFP mice were placed on a high fat or chow diet, or HFD fed mice underwent VSG or sham surgery. As expected, mice on HFD compared to chow diet showed increased body weight (Fig. 2A), fasting blood glucose and a blunted response to insulin in an insulin tolerance test (ITT, Fig. 2B). The slight increase in blood glucose at 15 min in the ITT due to stress was only seen in the HFD group. Separately, *gcg*-DTR-eGFP mice which had been on HFD and developed insulin resistance were divided into matched groups for sham or VSG surgery, in which the greater curvature of the stomach was removed to leave a tubular stomach (full details of the surgical procedure are outlined in 2.2.3). VSG resulted in significant body weight loss compared to sham (Fig. 2C), due to loss of fat but not lean mass (Fig. 2D). Food intake was reduced in VSG mice compared to shams for the entire 3 week follow-up period (Fig. 2E). VSG mice also showed improved glucose tolerance in a mixed meal tolerance test (intragastric gavage of Ensure plus liquid diet), with a faster clearance of glucose after reaching the same peak at 15 min (Fig. 2F). In a separate and independent cohort, VSG increased plasma GLP-1 concentrations following a glucose gavage 5 weeks post-surgery (Fig. 2G).

The colon and ileum of chow, HFD, sham and VSG treated *gcg*-DTR-eGFP mice were harvested and L cells, *gcg*-positive, (chow / HFD, n = 5,

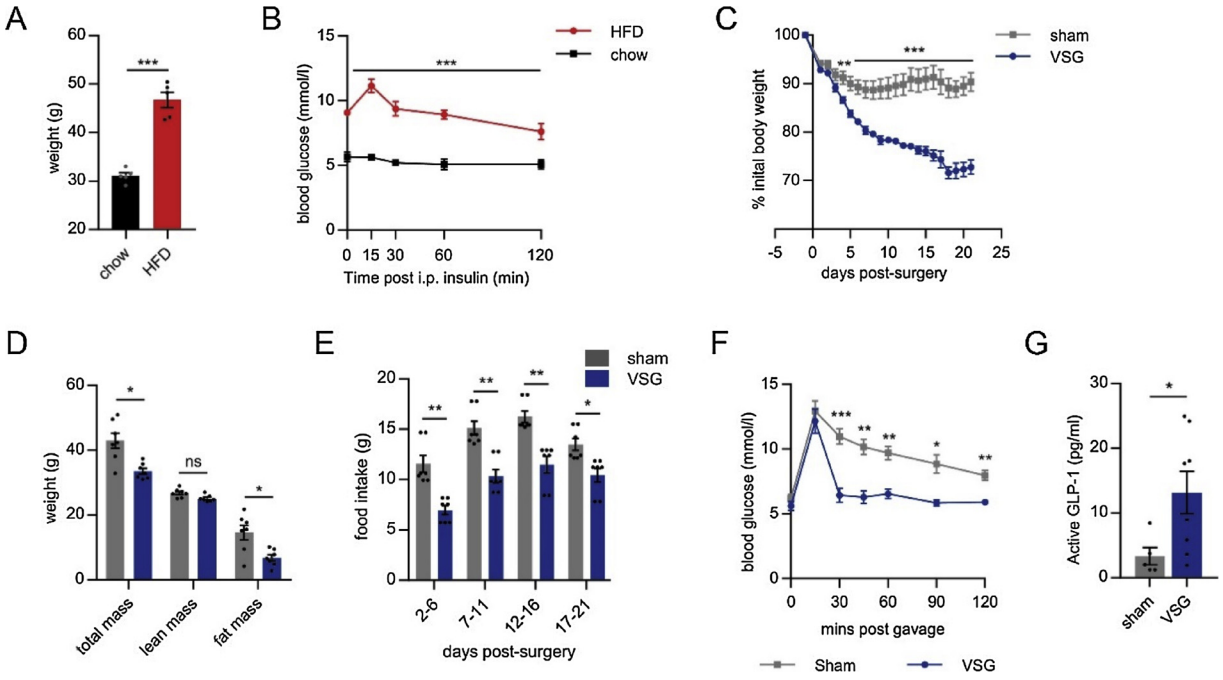

Fig. 2. Metabolic characterisation of the HFD/chow and VSG/sham cohorts. (A) Body weight at the time of L cell isolation by FACS, and (B) blood glucose following *i.p.* insulin injection of the HFD and chow mice used for L cell sequencing, n = 3 - 5. (C) % of initial body weight, (D) total, lean and fat mass 21 days post-surgery, (E) cumulative food intake per 5 days, and (F) blood glucose during a mixed meal tolerance test (gavage of Ensure) of the VSG and sham mice used for sequencing. (G) Active GLP-1 concentration in plasma following glucose gavage in an independent VSG cohort. n = 7 for all VSG/sham experiments, except (G) where n = 5 for sham and 8 for VSG. Mean ± SEM shown, significance calculated by Welch two sample *t*-test with multiple testing correction by Bonferroni method where relevant. * = $p < 0.05$, ** = $p < 0.01$, *** = $p < 0.001$.

16 weeks of diet) or L cells and epithelial cells, *gcg*-negative, (sham / VSG, n = 7, around 20 weeks pre-surgical HFD and 22–29 days post-surgery) were purified by FACS. No significant differences were observed in the number of L cells isolated in HFD vs. chow, or in the number or proportion of L cells in VSG vs. sham (Supplementary Information Fig. 1). Extracted RNA was used for bulk transcriptome sequencing to determine widespread and consistent changes in the L cell transcriptome in response to HFD or VSG. Cells from individual mice were purified and sequenced as separate samples. The sorting specificity of the sequenced samples was confirmed by the enrichment of *gcg* (Fig. 3A) and *pyy* (Fig. 3B) in colonic L cells compared to epithelial cells in both the VSG and sham cohorts. *gcg* was also significantly enriched in ileal L cells and *pyy* showed a strong trend towards L cell enrichment. Epithelial cells were not sorted from the HFD and chow cohorts, but *gcg* and *pyy* are in the top 60 expressed genes in all L cell cohorts (Fig. 3C). Other enteroendocrine hormones such as *cck* (Cholecystokinin), *nts* (Neurotensin), *sct* (Secretin) and *insl5* (Insulin-like 5) are also amongst the highest expressed genes in L cells (Fig. 3C).

Multidimensional scaling (MDS) of all 75 sequenced samples shows separation by tissue (colon vs. ileum) along the first dimension, and by cell type (epithelial vs. L cell) along the second dimension (Fig. 3D). This indicates that there are large differences in the L cell transcriptome along the GI tract with L cells clustering closer to their surrounding epithelial cells than L cells from other intestinal locations, particularly in the ileum. Nevertheless, the L cell retains some unique transcriptional characteristics (see section 3.4) which distinguish L cells from the average gut epithelial cell. No clear separation is seen between HFD and chow or VSG and sham samples.

3.3. The metabolic state does not widely effect the L cell transcriptome

A clustered heatmap of high variance genes from the HFD and chow L cells shows separation by tissue, but not by diet (Fig. 4A). To determine the effect of HFD on the L cell transcriptome, differentially expressed (DE) genes were identified for the HFD vs. chow comparison separately in the colon and ileum (Fig. 4B, genes listed in Supplementary Information Table 2). As indicated by the heat map, only a small number of DE genes were identified, none of which were DE in both tissues, showing that there is no consistent regulation of the general L cell transcriptome by chronic HFD. However, no DE genes being similarly regulated in both tissues may be due to over half of these diet regulated genes being tissue enriched in at least one ileum vs. colon comparison (Fig. 4C, L-TissDE$_{all}$ genes defined in Section 3.4). To determine the biological consequences of these changes following HFD, gene ontology (GO) biological process term enrichment was performed, comparing all DE genes in both tissues to a background of genes expressed in at least one HFD vs. chow comparison. This revealed that diet effected genes are primarily involved in immune related processes (Fig. 4D).

Similarly, a heatmap of all L cell VSG and sham samples shows separation by tissue but not surgery (Fig. 4E). The comparison of VSG vs. sham was calculated for each tissue but no genes reached the differential expression cut-off. To determine if this was due to large variation in weight loss of the sham cohort, probably due to some sham mice receiving a small reduction in stomach volume, VSG samples were compared to the three heaviest shams only, but still no DE genes were identified.

3.4. Large differences are seen between ileal and colonic L cell transcriptomes

As indicated by the MDS analysis (Fig. 3D), a heatmap clearly shows that the majority of the top variance L cell genes are differentially expressed between tissues (Fig. 5A). An ileum vs. colon comparison was made separately for each metabolic condition (HFD, chow, VSG and sham), identifying a large number of DE genes in all cases (838 – 1 600) with similar numbers of colonic and ileal enriched genes (Fig. 5B). The overlap between the DE genes identified shows many genes are

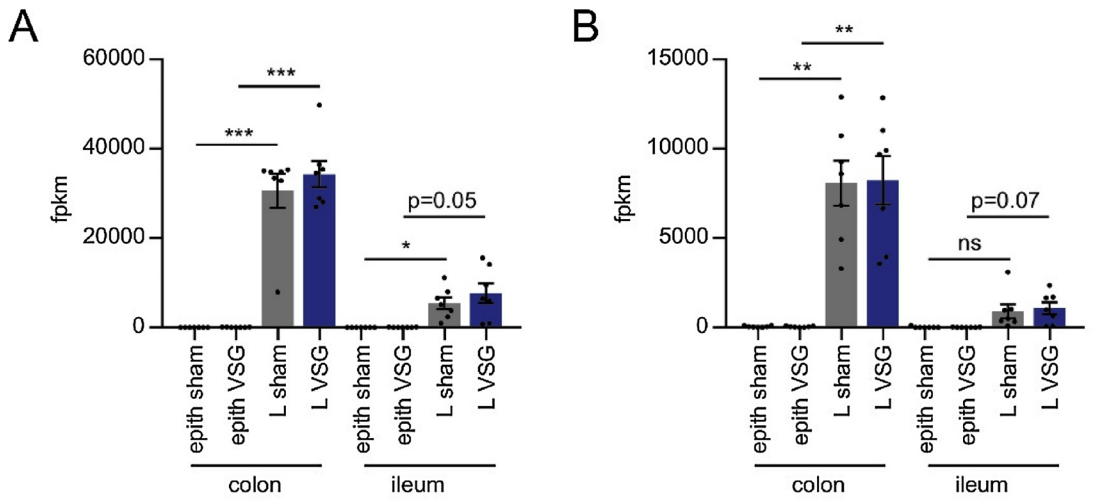

C

	HFD		Chow		VSG		Sham	
	Colon	Ileum	Colon	Ileum	Colon	Ileum	Colon	Ileum
Gcg	11	36	7	30	3	16	3	16
Pyy	17	60	16	53	12	35	13	45
Gip	21,047	2,490	20,881	3,365	19,015	2,877	17,326	8,919
Cck	237	697	53	344	24	37	32	74
Nts	46	245	38	145	67	147	58	91
Sct	106	108	41	83	52	46	45	46
Insl5	204	8,214	60	6,022	32	2,845	35	6,578

fpkm rank in sample

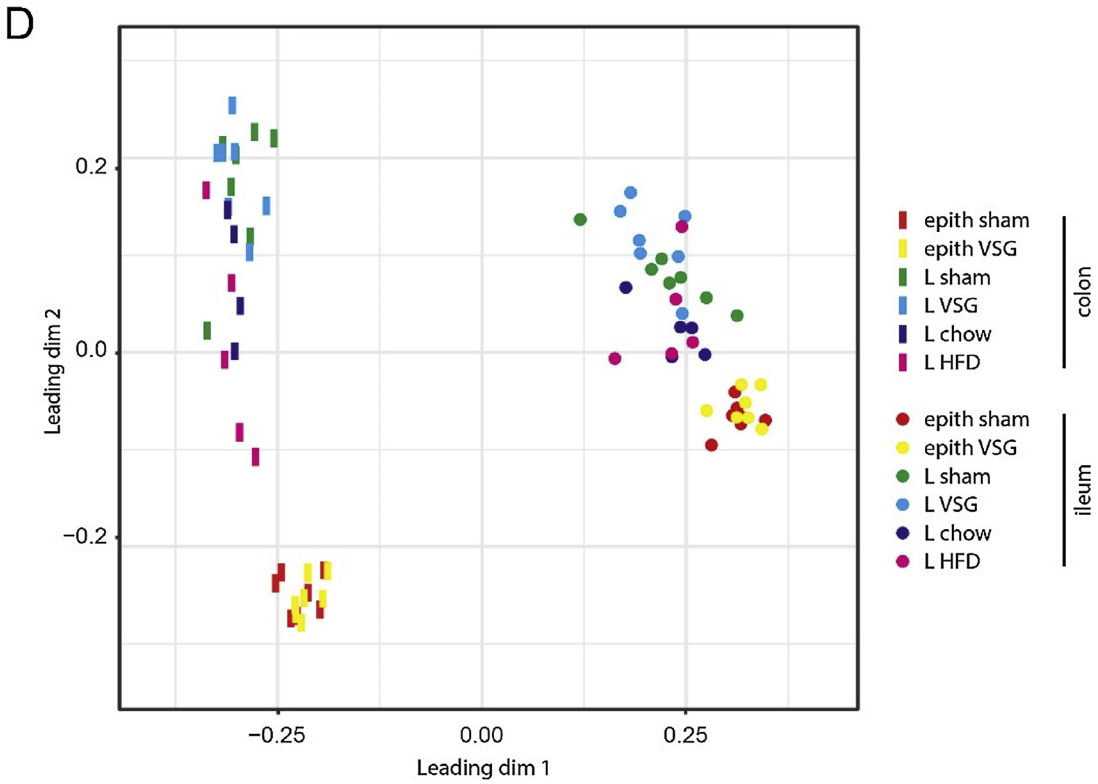

Fig. 3. Large tissue differences are seen in the whole L cell transcriptome. Fragments per kilobase of transcript per million mapped reads (fpkm) of (A) *gcg* and (B) *pyy* in sequenced L and epithelial cells (n = 7). Mean ± SEM shown, significance calculated by Welch two sample *t*-test with multiple testing correction by Bonferroni method, * = $p < 0.05$, ** = $p < 0.01$, *** = $p < 0.001$. (C) The rank of genes encoding enteroendocrine hormones in all L cell cohorts when all genes are ordered by average fpkm. (D) Multidimensional scaling of all 75 samples used for transcriptome analysis.

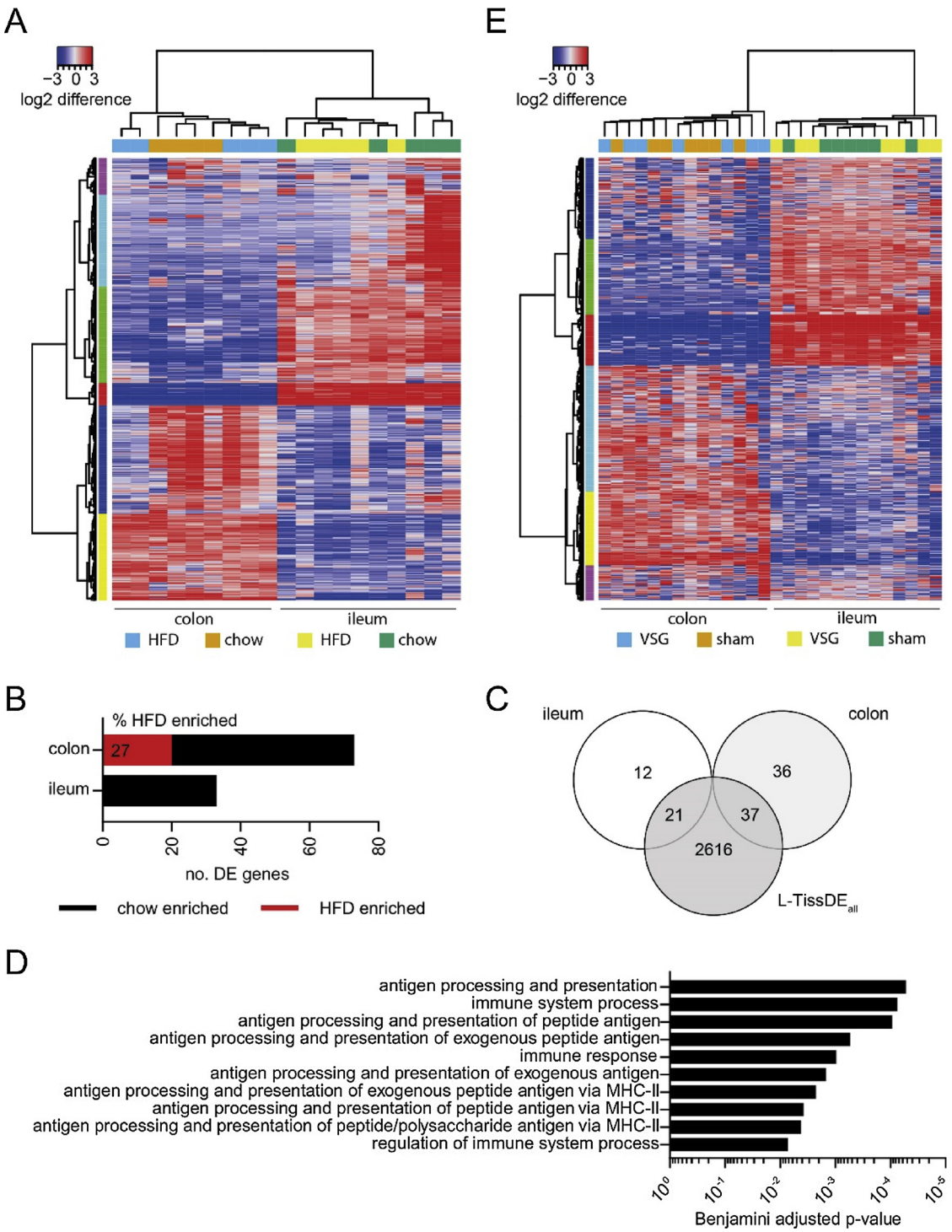

Fig. 4. The effect of HFD induced insulin resistance and VSG surgery on the L cell transcriptome. (A) Heatmap of top 1000 high variance genes across all HFD and chow samples, with genes and samples ordered by hierarchical clustering. (B) Number of DE genes and their direction of regulation for the HFD vs. chow comparison. (C) Overlap of diet regulated genes from the ileum and colon and all genes enriched in at least one colon vs. ileum comparison. (D) Top 10 enriched GO process terms for all DE genes in the HFD vs. chow comparison. (E) Heatmap of top 1000 high variance genes across all VSG and sham L cell samples, with genes and samples ordered by hierarchical clustering.

consistently tissue enriched, with 293 defined as DE genes in all 4 comparisons and an additional 313 being regulated in 3 of the 4 metabolic conditions (L-TissDE$_{const}$, Fig. 5C, genes listed in Supplementary Information Table 3). In all cases, these 606 consistently regulated genes are enriched in the same tissue in all significant comparisons, showing the differences seen are robust and consistent across the two independent experiments. The 2 674 genes DE in at least one metabolic condition are defined as L-TissDE$_{all}$.

GO enrichment analysis of the L-TissDE$_{const}$ genes (compared to a background of genes expressed in at least 3 of the 4 comparisons), revealed a high enrichment in genes involved in transport (Fig. 5D), and similarly KEGG pathway analysis showed the largest enrichment in protein and fat digestion and absorption (Fig. 5E). Separate analyses of genes enriched in the ileum and colon indicated that the observed

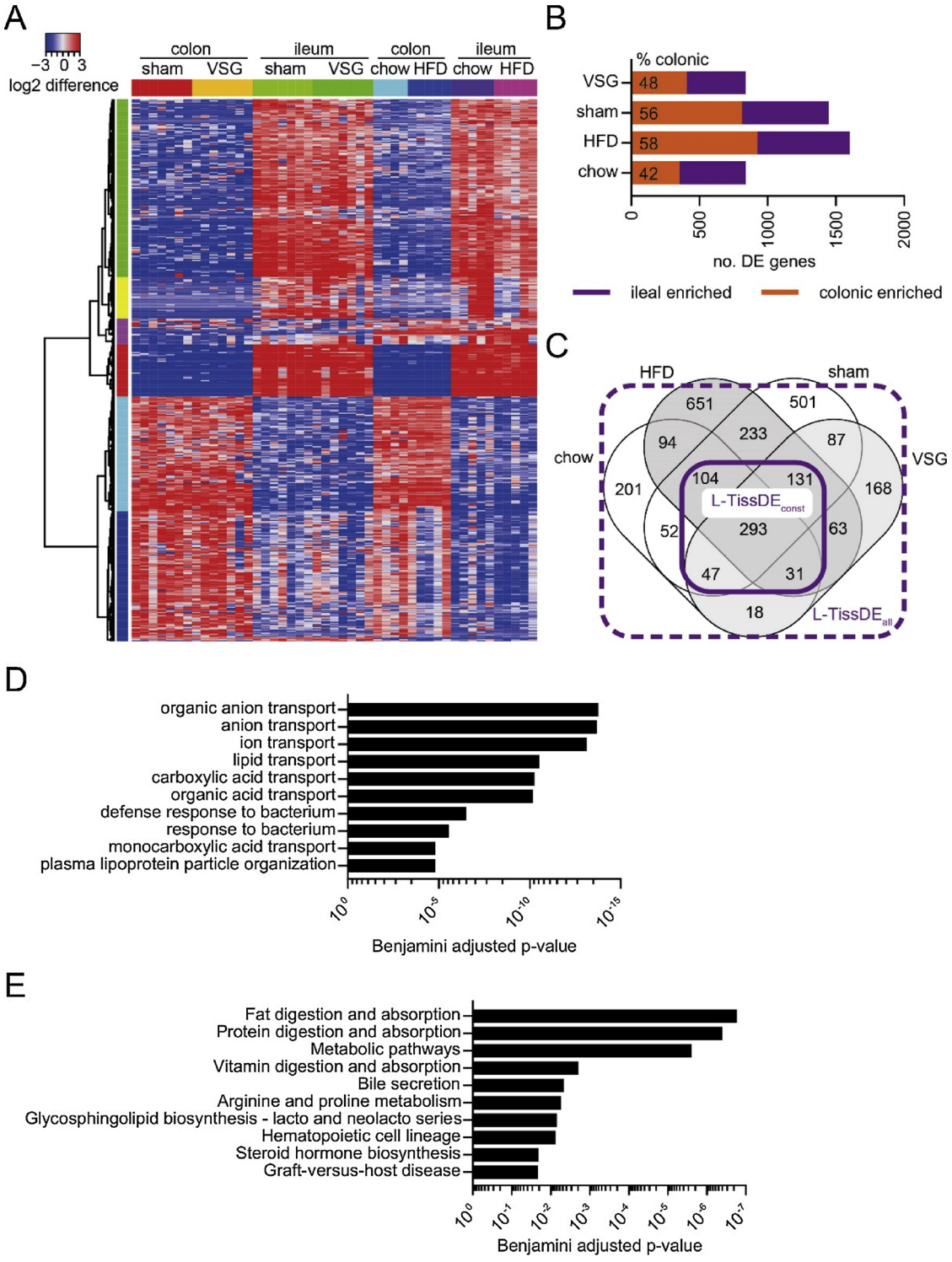

Fig. 5. Comparison of colonic and ileal L cell transcriptomes. (A) Heatmap of top 500 high variance genes across all L cell samples, genes arranged by hierarchical clustering and samples ordered by condition. (B) Number of DE genes and their direction of regulation for ileum vs. colon comparisons. (C) Overlap of differentially expressed genes per condition. The purple squares highlight the consistently regulated genes used for further enrichment analyses. (D) GO process enrichment and (E) KEGG pathway enrichment of L-TissDE$_{const}$ genes.

enrichments were driven by ileal enriched genes (Supplementary Information Fig. 2). Thus, ileal L cells are enriched for dietary nutrient transport genes, in line with the increased presence of luminal nutrients in this region. In addition, several enteroendocrine hormones are differentially expressed between tissues with *gcg*, *pyy*, *ppy* and *insl5* enriched in the colon in at least one comparison, and *gip* in the ileum. The degree of enrichment varies, with *gcg* being only slightly enriched compared to *insl5* which is almost specific to the colonic L cell.

3.5. Epithelial cells differ between the colon and ileum in a similar way to L cells, with L cells being defined by a small distinct subset of genes

As L cell tissue differences are primarily due to genes involved in nutrient transport, and the MDS analysis (Fig. 3D) indicated similarities

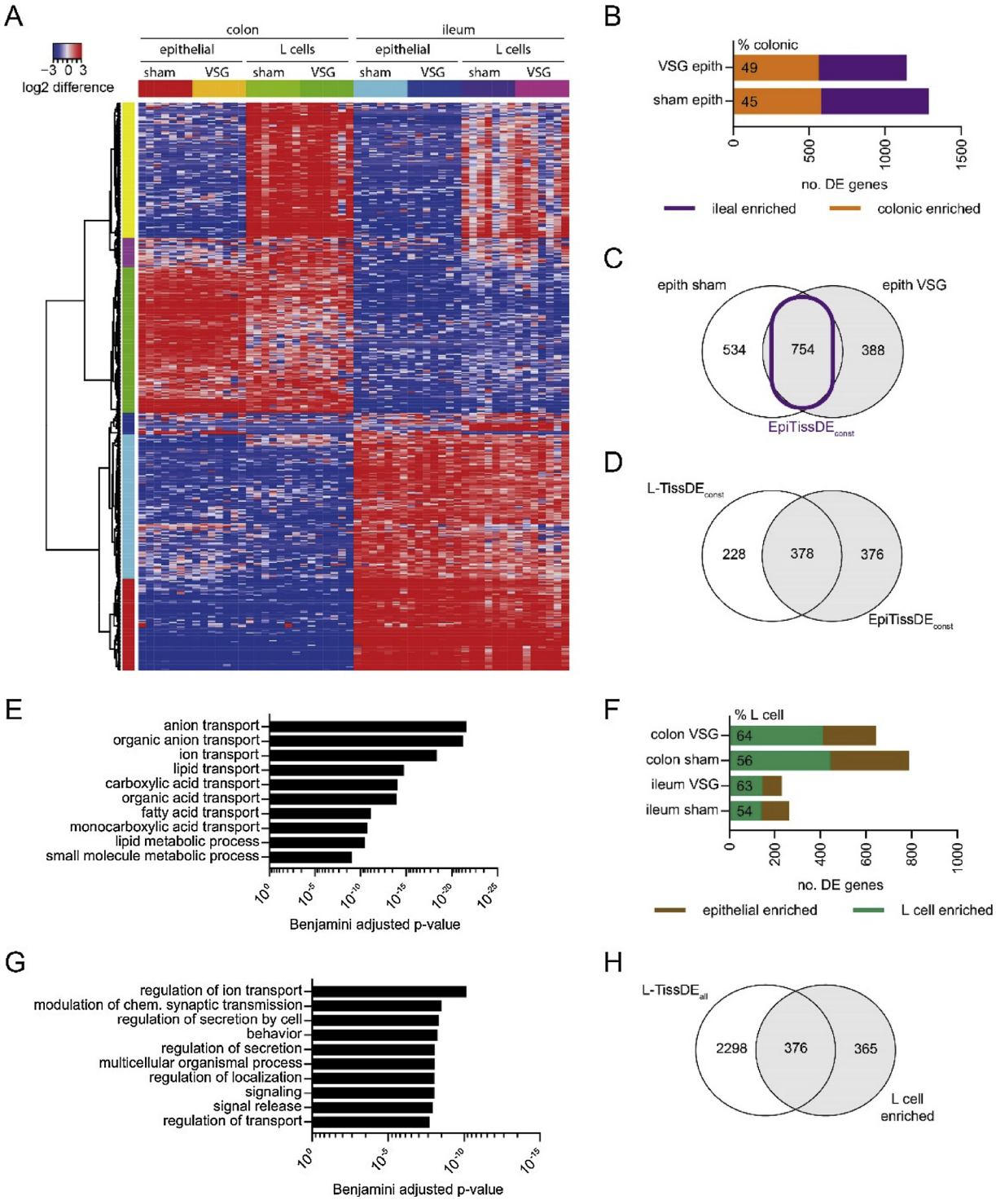

Fig. 6. L cell tissue specificity in the context of epithelial cells. (A) Heatmap of top 500 high variance genes in VSG/sham L cell and epithelial cell samples, genes arranged by hierarchical clustering and samples ordered by condition. (B) Number of DE genes and their direction of regulation for the ileum vs. colon comparison of epithelial cells. (C) Overlap of these DE genes, the consistently tissue enriched genes used for enrichment analyses are highlighted in the purple box. (D) Overlap of consistently tissue enriched genes in L cells (L-TissDE$_{const}$) and epithelial cells (EpiTissDE$_{const}$). (E) GO process enrichment of the EpiTissDE$_{const}$ genes. (F) Number of DE genes and their direction of regulation for the L cell vs. epithelial cell comparison. (G) GO process enrichment of all L cell enriched genes. (H) Overlap of L cell enriched and tissue enriched genes (L-TissDE$_{all}$).

to epithelial cells, we investigated to what extent the tissue differences in L cells recapitulate differences in the surrounding epithelium and which are specific to the L cell. Clustering of the top variance genes shows many genes are similarly tissue enriched in epithelial and L cells, but a subset of genes are differentially expressed between L cells and epithelial cells from the same tissue (yellow cluster, Fig. 6A). DE genes were defined for the ileum vs. colon comparison of epithelial cells from VSG and sham, and again a large number of genes (1 142 – 1 288) were identified with similar numbers regulated in each direction (Fig. 6B). The overlap between the VSG and sham comparisons gives 754 consistently tissue enriched genes, only one of which is enriched in different tissues in each condition (EpiTissDE$_{const}$, Fig. 6C, genes listed in

Supplementary Information Table 4). Together, this confirms that epithelial cells also differ widely and consistently between the ileum and colon.

There is a large overlap between the L-TissDE$_{const}$ and EpiTissDE$_{const}$ genes (Fig. 6D), with all the overlapping genes being enriched in the same tissue. Additionally, GO process term enrichment of EpiTissDE$_{const}$ genes shows the greatest enrichment in terms associated with transport similarly to the L cell (Figs. 5D and 6 E), and confirming that the tissue differences in the L cell transcriptome largely reflect the local environment with L cells recapitulating many properties of the surrounding epithelium. Again, the enrichment in GO terms associated with transport is driven by ileal enriched genes, but, in contrast to L cells, the colonic enriched genes also show a slight enrichment in transport associated terms (Supplementary Information Fig. 3), reflecting the specialised role of enterocytes which constitute the majority of intestinal epithelial cells.

To identify which genes distinguish L cells from the surrounding epithelium, DE genes were identified for the L cell vs. epithelial comparison for the VSG and sham cohorts per tissue (Fig. 6F). Many DE genes were identified showing that L cells are transcriptionally distinct from the majority of intestinal epithelial cells. A larger number of DE genes were identified from the colonic samples, showing that colonic L cells are more distinct from the surrounding cells, as indicated by the MDS plot in Fig. 3D. GO process term enrichment of the genes L cell enriched in at least one comparison (green bars in Fig. 6F) shows L cells are enriched in genes involved in ion transport, and the regulation of secretion and signalling compared to the surrounding epithelial cells (Fig. 6G). To determine which L cell enriched genes are differentially expressed between tissues, the overlap between these L cell enriched genes and L-TissDE$_{all}$ genes was determined. Around half of the L cell enriched genes are tissue enriched (Fig. 6H, genes listed in Supplementary Information Table 5), showing that even the genes which define an L cell vary along the length of the gut and that not all the tissue specificity of L cells is due to similarities with the local epithelial transcriptome. 306 of the 376 tissue enriched L cell enriched genes are colonically enriched, again confirming that colonic L cells are more distinct from the epithelium. Selected L cell enriched tissue enriched genes are listed in Table 1. In contrast, the 365 L cell enriched genes that are not tissue specific can be used as more generally applicable markers for L cells (genes listed in Supplementary Information Table 6), although we cannot rule out the expression of these in small numbers of non-L cells.

3.6. L cells from different regions differ in sensitivity to GLP-1 secretagogues

To confirm that these differences in nutrient transporter and hormone receptor expression between the ileum and colon affect regulation of GLP-1 secretion from L cells, primary mixed cultures of crypts isolated from the ileum and colon were stimulated and the proportion of GLP-1 secreted determined. *Slc5a1*, encoding the sodium-glucose transporter SGLT1, and *slc15a1*, encoding the peptide transporter PEPT1, were identified as enriched in the ileum in L cells from all metabolic conditions. In contrast, *avpr1b*, the receptor for vasopressin, was identified as enriched in the colon in two comparisons. Fig. 7A shows the fpkms of these genes in L cells, all of which have been shown to be involved in the regulation of GLP-1 secretion [36–38]. Colonic crypts secreted a greater proportion of their GLP-1 content than ileal cells under unstimulated conditions, did not respond to stimulation by glucose, and were strongly simulated by arginine-vasopressin. In contrast, ileal crypts were stimulated by glucose and only showed a mild induction by arginine-vasopressin (Fig. 7B). The non-hydrolysable dipeptide glycyl-sarcosine (gly-sar), which acts through PEPT1, also stimulates ileal cells to a greater extent as predicted. Taken together, this confirms that ileal and colonic L cells respond differently to physiological stimuli.

Table 1
Hormones, transporters and GPCRs from the 376L cell enriched tissue enriched genes.

Hormones	GPCRs	Transporters		
Insl5	*Avpr1b*	*Slc8a1*	*Scn3a*	*Rims2*
Ppy	*Gprc5c*	*Kcnk3*	*Pea15a*	*Slc12a2*
Gcg	*Adgrl1*	*Abcc1*	*Kcnh2*	*Cacna1c*
Pyy	*Chml*	*Slco3a1*	*Abcc8*	*Asic2*
	Gpr119	*Slc29a4*	*Kif5c*	*Nup210*
	Sstr5	*Stard5*	*Kcnb1*	*Gga2*
	Hcar2	*Slc6a19*	*Cadps*	*Atp1a3*
	Celsr3	*Itpr1*	*Hap1*	*Apoe*
	Agtr1a	*Esyt1*	*Grik5*	*Dync1i1*
	Cmklr1	*Stxbp1*	*Scg5*	*Gpm6b*
	P2ry13	*Tmed8*	*Ap3b2*	*Mcoln3*
	Gpr179	*Sv2c*	*Ryr3*	*Ramp2*
		Lrrc8c		

4. Discussion

The L cell and GLP-1 are established drug targets for the treatment of T2DM, but both L cell heterogeneity and the changes L cells undergo during the development of diabetes and its resolution following bariatric surgery are not well understood. We report the development of the *gcg*-DTR-eGFP mouse line, a L cell reporter line generated independently of the *gcg*-Venus mouse published by Reimann et al. [36], and an alternative cell isolation procedure which is specific for epithelial cells. This enabled the transcriptomic characterisation by RNA sequencing of FACS isolated L cells, here defined as *gcg*-expressing cells, and the surrounding epithelial cells after HFD (L cells only) and VSG. We focused on the changes following HFD and VSG, the differences between L cells from different tissues (ileum and colon), and the similarities and differences between L cells and the surrounding epithelium.

As expected, HFD led to increased body weight, elevated fasting blood glucose and the development of insulin resistance, with VSG resulting in body fat loss, improved glucose tolerance and increased postprandial circulating GLP-1. As the HFD and VSG experiments were not performed in parallel the metabolic characteristics cannot be directly compared, so an ITT was not performed in the VSG cohort to minimise stress and enable the characterisation of the L cell transcriptome at a relatively early timepoint post-surgery. Given the phenotypes we observed, we were surprised that the L cell transcriptome showed only small changes after HFD and was not significantly altered following VSG. There was no significant regulation of *gcg* or proteins known to be involved in the regulation and secretion of GLP-1, so, in our hands, transcriptional changes in ileal and colonic L cells cannot explain the influence of HFD or VSG on GLP-1 secretion. As we performed bulk sequencing, changes in a subset of L cells in response to HFD or VSG cannot be ruled out, but to contribute to the observed physiological effects we would expect a widespread and consistent response in the majority of L cells, or at least an effect strong enough to influence bulk results. Our findings are in contrast to the work of Richards et al. who describe reduced expression of L cell specific genes following HFD [12], possibly as they used the whole SI in their long term experiments or due to methodological differences such as tissue preparation methods and time of day of harvest. However, as here we sequenced mice with elevated fasting blood glucose, our findings are in line with Dusaulcy et al. who observed that L cells from hyperglycaemic HFD mice have a molecular footprint similar to low fat diet mice, in contrast to normoglycaemic HFD mice [10].

DE genes after HFD were enriched for those associated with immune related processes. Previously, the L cell has been shown to respond to and contribute to immune activation and gut inflammation. Lipopolysaccharide (LPS) administration and manipulation of gut barrier integrity trigger GLP-1 secretion [39], GLP-2 enhances intestinal barrier function [40,41], and GLP-1 receptors regulate intestinal

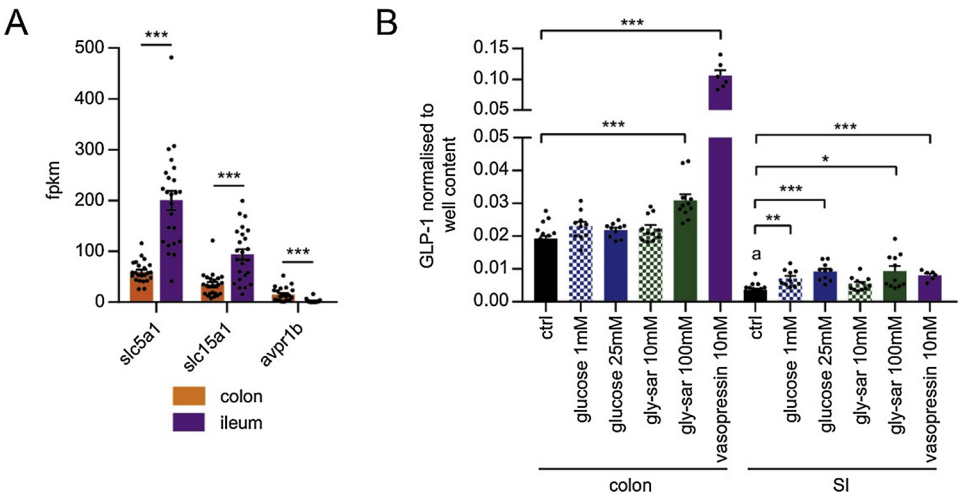

Fig. 7. L cells respond differently to GLP-1 secretagogues dependent on their location in the GI tract. (A) Average fpkm of selected genes from all L cell sequenced samples (chow, HFD, sham, VSG), n = 23 for colon and 24 for ileum. Significance calculated with Welch two sample *t*-test adjusted for multiple testing with Bonferroni correction, *** = $p < 0.001$. (B) Active GLP-1 secreted normalised to GLP-1 content of well, ctrl (unstimulated) n = 18 from 3 mice, glucose n = 10 from 3 mice, gly-sar n = 11 from 3 mice, arginine vasopressin n = 6 from 2 mice. Significance calculated with Welch two sample *t*-test, ** = $p < 0.01$, *** = $p < 0.001$ for comparison to control from the same tissue adjusted for multiple testing with Bonferroni correction, a = $p < 0.001$ for comparison between ctrl from colon and ileum. In all cases, mean ± SEM shown.

epithelial lymphocytes [42]. Here, several major histocompatibility complex (MHC) genes were downregulated by HFD, such as *H2-K1* in the colon, indicating that antigen presentation by the L cell, a key sensor of luminal content, is altered by HFD. As L cells are able to sense directly the external and immunotolerant environment of the intestinal lumen, this regulation of MHC genes by HFD may contribute to the chronic inflammation commonly associated with obesity.

The absence of significant regulation of the L cell transcriptome following VSG indicates that, under the measured conditions, changes in GLP-1 secretion occur without a major resetting of the transcriptional profile of distal L cells. Thus, if VSG regulates GLP-1 secretion from these cells it does so at the protein level, or elevated GLP-1 secretion simply occurs due to changes in luminal nutrient content and absorption following VSG resulting from increased rates of gastric emptying and intestinal transit [43]. Alternatively, altered circulating GLP-1 may be due to transcriptional changes in proximal L cells or, more unlikely, pancreatic α-cells. To date, no comparable data on the L cell transcriptome following bariatric surgery has been published, so to confirm the general applicability of our findings experiments including the proximal intestine, additional time-points post-surgery and different surgical procedures such as Roux-en-Y gastric bypass are required.

In contrast to the effects of diet and surgery, large differences were observed between ileal and colonic cells, which were fairly consistent across the two independent experiments. Previously, selected L cell related genes have been shown to be differentially expressed along the length of the gut [3,36,44], but here we have performed an analysis of the complete transcriptome, and considered L cell tissue differences in the context of the surrounding epithelium. Additionally, we identified a large number of genes enriched in L cells compared to the general epithelium, both tissue enriched and those which are not differentially expressed between tissues, which could be used as alternative L cell or enteroendocrine cell (EEC) markers. Both MDS analysis and the numbers of DE genes indicated that L cells are transcriptionally more similar to their surrounding epithelial cells than to L cells from a different region of the gut. As per the classic definition of an L cell, FACS purified L cells showed high expression and enrichment of both *gcg* and *pyy*. Several additional hormones were also highly expressed, including *cck*, *nts* and *sct*, confirming in a further mouse model the widespread overlap of enteroendocrine hormone expression in L cells as previously reported [3,45–47]. Enteroendocrine hormones display expression gradients along the GI tract [1] which is classically due to different gradients of each enteroendocrine cell type. However, we observe that several hormones are differentially expressed within L cells, such as the colonic enrichment of *gcg*, *pyy* and *insl5* and ileal enrichment of *gip* which is in agreement with the work of Habib et al. [3], except INSL5 was not included in their study. A trend towards *gcg* enrichment in colonic L cells was also observed by Suzuki et al. [44], but they observed increased *pyy* expression in SI cells in contrast to our work and that of Habib et al. Here, the expression of *pcsk1* or *pcsk2* was not significantly different between tissues, suggesting no large differences in the processing of Preproglucagon.

L cells secrete hormones in response to luminal nutrients sensed by GPCRs or through electrogenic transporters [48]. GO process and KEGG pathway enrichment analyses showed that the transcriptomic differences between ileal and colonic L cells are primarily driven by ileal enrichment of genes involved in nutrient transport and metabolism, including several proteins known to regulate the L cell response to nutrients. For example, *slc5a1* and *slc15a1* are involved in the L cell response to glucose and di/tripeptides respectively [36,37] and are consistently ileal enriched. Published data showed that glucose stimulated GLP-1 responses are increased in the rat SI compared to the colon [49] and here we confirmed that ileal L cells secrete GLP-1 in response to glucose and the non-hydrolysable gly-sar dipeptide to a greater extent than colonic cells, as predicted by the differential gene expression. The absence of regulation by dietary nutrients of GLP-1 secretion by colonic L cells has also been indicated by recent work showing the co-secretion and thus co-regulation of GLP-1, PYY and INSL5 secretion from colonic L cells, despite circulating levels of INSL5 being increased upon caloric restriction in contrast to postprandial elevations in GLP-1 [50]. Although we only confirmed the effect of glucose and gly-sar on GLP-1 secretion in primary cells, the transcriptomic data, distribution of dietary nutrients in the GI tract and recent publications indicate that there are widespread tissue differences in the response to dietary nutrients such that ileal L cells contribute more to postprandial GLP-1 secretion than colonic cells. In contrast, our gene expression data indicates a role of colonic cells in the response to non-dietary luminal metabolites. *ffar2* (GPCR43), which induces GLP-1 secretion in response to the short chain fatty acids produced by microbiota from dietary fibre in the distal lumen [51,52], is enriched in the colon in one cohort.

The potential of the L cell to respond to circulatory and not solely luminal stimuli has recently been illustrated. Arginine vasopressin has been shown to act through *avpr1b* in colonic L cells to induce GLP-1 and PYY secretion, which may contribute to intestinal fluid homeostasis as PYY reduces colonic water and anion secretion [38], and GLP-1 has been implicated in a putative gut-renal axis regulating postprandial fluid and electrolyte homeostasis [53]. We showed that arginine vasopressin stimulated GLP-1 secretion from colonic cells to a greater extent than ileal cells, likely due to the differential expression of *avpr1b* which is enriched in the colon in the HFD and chow cohorts. We also observed that colonic L cells basally secrete a greater proportion of their GLP-1. Together, this indicates that the primary role of GLP-1 secretion by

colonic L cells is not the control of postprandial glucose homeostasis but rather a contribution to basal levels of GLP-1 and other aspects of homeostasis. Nevertheless, colonic L cells may contribute to glucose homeostasis through the secretion of other hormones, for example the colon specific INSL5 which promotes appetite and hepatic glucose production during periods of energy deprivation [54,55]. In general, our data indicates that L cells from different regions of the GI tract contribute differently to whole organism metabolism, by responding to different luminal metabolites, secreting different hormones, and reacting with different kinetics as metabolites arrive at different times post-ingestion.

Here we performed bulk RNA sequencing as the primary aim was to identify the changes which occur following HFD and VSG in a consistent manner across all L cells. However, to explore L cell heterogeneity in more detail, sequencing of single L cells is required and has recently been used to highlight the transcriptional heterogeneity of L cells within a single intestinal region. Glass et al. focused on *gcg*-expressing cells from the upper SI and classified L cells into three transcriptional clusters each with a distinct profile of hormone expression [56], and Haber et al. performed clustering of all SI epithelial cells to redefine enteroendocrine cell types with both SILA and SIL-P cells expressing both *pyy* and *gcg* [57]. The tissue differences we observe suggest that additional L cell / enteroendocrine transcriptional clusters exist in the distal gut with the composition of the heterogeneous L cell population changing along the gut axis. Furthermore, L cells have been shown to alter their hormonal profile as they migrate along the crypt-villus axis [58], adding to the complexity of L cell heterogeneity. There remains a requirement for a better understanding of this heterogeneity along the GI tract and the subsequent development of a new EEC classification to reflect this. Clinically, this heterogeneity will have implications on the effects and efficacy of novel anti-diabetic drugs, so the specific transcriptome of the subset of L cells expressing target proteins should be considered during drug development.

Author contributions

KAR designed and performed experiments, analysed data and wrote the manuscript. MA performed the VSG and sham surgeries. ES co-ordinated and supervised the library preparation and RNA sequencing. LO processed the sequencing data and performed the differential expression analysis. HN and SW designed and supervised the project and assisted with the manuscript. All authors approved the final manuscript.

Acknowledgements

The authors acknowledge the assistance and support of the Flow Cytometry Facility, University of Zurich for their assistance in performing the cell sorting experiments, and Tobias Hildebrandt and Werner Rust for the library preparation and RNA sequencing. Financial support was provided by Boehringer Ingelheim Fonds and ETH Zurich.

Appendix A. Supplementary data

Supplementary material related to this article can be found, in the online version, at doi:https://doi.org/10.1016/j.peptides.2019.01.001.

References

[1] K. Sjolund, G. Sanden, R. Hakanson, F. Sundler, Endocrine cells in human intestine: an immunocytochemical study, Gastroenterology 85 (5) (1983) 1120–1130.
[2] D.J. Drucker, The biology of incretin hormones, Cell Metab. 3 (3) (2006) 153–165.
[3] A.M. Habib, P. Richards, L.S. Cairns, G.J. Rogers, C.A. Bannon, H.E. Parker, T.C. Morley, G.S. Yeo, F. Reimann, F.M. Gribble, Overlap of endocrine hormone expression in the mouse intestine revealed by transcriptional profiling and flow cytometry, Endocrinology 153 (7) (2012) 3054–3065.
[4] T. Vilsboll, T. Krarup, C.F. Deacon, S. Madsbad, J.J. Holst, Reduced postprandial concentrations of intact biologically active glucagon-like peptide 1 in type 2 diabetic patients, Diabetes 50 (3) (2001) 609–613.
[5] K. Faerch, S.S. Torekov, D. Vistisen, N.B. Johansen, D.R. Witte, A. Jonsson, O. Pedersen, T. Hansen, T. Lauritzen, A. Sandbaek, J.J. Holst, M.E. Jorgensen, GLP-1 response to oral glucose is reduced in prediabetes, screen-detected type 2 diabetes, and obesity and influenced by sex: the ADDITION-PRO study, Diabetes 64 (7) (2015) 2513–2525.
[6] M. Nauck, F. Stockmann, R. Ebert, W. Creutzfeldt, Reduced incretin effect in type 2 (non-insulin-dependent) diabetes, Diabetologia 29 (1) (1986) 46–52.
[7] M.P. Larsen, S.S. Torekov, Glucagon-like peptide 1: a predictor of type 2 diabetes? J. Diabetes Res. 2017 (2017) 13.
[8] M.A. Nauck, I. Vardarli, C.F. Deacon, J.J. Holst, J.J. Meier, Secretion of glucagon-like peptide-1 (GLP-1) in type 2 diabetes: what is up, what is down? Diabetologia 54 (1) (2011) 10–18.
[9] T. Aranias, A. Grosfeld, C. Poitou, A.A. Omar, M. Le Gall, S. Miquel, K. Garbin, A. Ribeiro, J.L. Bouillot, A. Bado, E. Brot-Laroche, K. Clement, A. Leturque, S. Guilmeau, P. Serradas, Lipid-rich diet enhances L-cell density in obese subjects and in mice through improved L-cell differentiation, J. Nutr. Sci. 4 (2015) e22.
[10] R. Dusaulcy, S. Handgraaf, S. Skarupelova, F. Visentin, C. Vesin, M. Heddad-Masson, F. Reimann, F. Gribble, J. Philippe, Y. Gosmain, Functional and molecular adaptations of enteroendocrine L-cells in male obese mice are associated with preservation of pancreatic alpha-cell function and prevention of hyperglycemia, Endocrinology 157 (10) (2016) 3832–3843.
[11] C. Kappe, Q. Zhang, T. Nyström, Å. Sjöholm, Effects of high-fat diet and the anti-diabetic drug metformin on circulating GLP-1 and the relative number of intestinal L-cells, Diabetol. Metab. Syndr. 6 (2014) 70-70.
[12] P. Richards, R. Pais, A.M. Habib, C.A. Brighton, G.S. Yeo, F. Reimann, F.M. Gribble, High fat diet impairs the function of glucagon-like peptide-1 producing L-cells, Peptides 77 (2016) 21–27.
[13] G. Mingrone, S. Panunzi, A. De Gaetano, C. Guidone, A. Iaconelli, G. Nanni, M. Castagneto, S. Bornstein, F. Rubino, Bariatric-metabolic surgery versus conventional medical treatment in obese patients with type 2 diabetes: 5 year follow-up of an open-label, single-centre, randomised controlled trial, Lancet (London, England) 386 (9997) (2015) 964–973.
[14] M. Rizzello, F. Abbatini, G. Casella, G. Alessandri, A. Fantini, F. Leonetti, N. Basso, Early postoperative insulin-resistance changes after sleeve gastrectomy, Obes. Surg. 20 (1) (2010) 50–55.
[15] A.K. McGavigan, D. Garibay, Z.M. Henseler, J. Chen, A. Bettaieb, F.G. Haj, R.E. Ley, M.L. Chouinard, B.P. Cummings, TGR5 contributes to glucoregulatory improvements after vertical sleeve gastrectomy in mice, Gut 66 (2) (2017) 226–234.
[16] A. Yousseif, J. Emmanuel, E. Karra, Q. Millet, M. Elkalaawy, A.D. Jenkinson, M. Hashemi, M. Adamo, N. Finer, A.G. Fiennes, D.J. Withers, R.L. Batterham, Differential effects of laparoscopic sleeve gastrectomy and laparoscopic gastric bypass on appetite, circulating acyl-ghrelin, peptide YY3-36 and active GLP-1 levels in non-diabetic humans, Obes. Surg. 24 (2) (2014) 241–252.
[17] M. Nannipieri, S. Baldi, A. Mari, D. Colligiani, D. Guarino, S. Camastra, E. Barsotti, R. Berta, D. Moriconi, R. Bellini, M. Anselmino, E. Ferrannini, Roux-en-Y gastric bypass and sleeve gastrectomy: mechanisms of diabetes remission and role of gut hormones, J. Clin. Endocrinol. Metab. 98 (11) (2013) 4391–4399.
[18] J.B. Cavin, A. Couvelard, R. Lebtahi, R. Ducroc, K. Arapis, E. Voitellier, F. Cluzeaud, L. Gillard, M. Hourseau, N. Mikail, L. Ribeiro-Parenti, N. Kapel, J.P. Marmuse, A. Bado, M. Le Gall, Differences in alimentary glucose absorption and intestinal disposal of blood glucose after Roux-en-Y gastric bypass vs sleeve gastrectomy, Gastroenterology 150 (2) (2016) 454-64.e9.
[19] M.B. Mumphrey, Z. Hao, R.L. Townsend, L.M. Patterson, H.R. Berthoud, Sleeve gastrectomy does not cause hypertrophy and reprogramming of intestinal glucose metabolism in rats, Obes. Surg. 25 (8) (2015) 1468–1473.
[20] A.P. Chambers, E.P. Smith, D.P. Begg, B.E. Grayson, S. Sisley, T. Greer, J. Sorrell, L. Lemmen, K. LaSance, S.C. Woods, R.J. Seeley, D.A. D'Alessio, D.A. Sandoval, Regulation of gastric emptying rate and its role in nutrient-induced GLP-1 secretion in rats after vertical sleeve gastrectomy, American journal of physiology, Endocrinol. Metab. 306 (4) (2014) E424–E432.
[21] A.P. Chambers, L. Jessen, K.K. Ryan, S. Sisley, H.E. Wilson-Perez, M.A. Stefater, S.G. Gaitonde, J.E. Sorrell, M. Toure, J. Berger, D.A. D'Alessio, S.C. Woods, R.J. Seeley, D.A. Sandoval, Weight-independent changes in blood glucose homeostasis after gastric bypass or vertical sleeve gastrectomy in rats, Gastroenterology 141 (3) (2011) 950–958.
[22] H.E. Wilson-Perez, A.P. Chambers, K.K. Ryan, B. Li, D.A. Sandoval, D. Stoffers, D.J. Drucker, D. Perez-Tilve, R.J. Seeley, Vertical sleeve gastrectomy is effective in two genetic mouse models of glucagon-like Peptide 1 receptor deficiency, Diabetes 62 (7) (2013) 2380–2385.
[23] A. Jimenez, A. Mari, R. Casamitjana, A. Lacy, E. Ferrannini, J. Vidal, GLP-1 and glucose tolerance after sleeve gastrectomy in morbidly obese subjects with type 2 diabetes, Diabetes 63 (10) (2014) 3372–3377.
[24] M.A. Nauck, M.M. Heimesaat, C. Orskov, J.J. Holst, R. Ebert, W. Creutzfeldt, Preserved incretin activity of glucagon-like peptide 1 [7-36 amide] but not of synthetic human gastric inhibitory polypeptide in patients with type-2 diabetes mellitus, J. Clin. Invest. 91 (1) (1993) 301–307.
[25] M. Rosenwald, A. Perdikari, T. Rulicke, C. Wolfrum, Bi-directional interconversion of brite and white adipocytes, Nat. Cell Biol. 15 (6) (2013) 659–667.
[26] T. Johansson, I. Broll, T. Frenz, S. Hemmers, B. Becher, H.U. Zeilhofer, T. Buch, Building a zoo of mice for genetic analyses: a comprehensive protocol for the rapid generation of BAC transgenic mice, Genesis (New York, N.Y. : 2000) 48 (4) (2010) 264–280.
[27] T. Rulicke, Pronuclear microinjection of mouse zygotes, Methods Mol. Biol. (Clifton, N.J.) 254 (2004) 165–194.
[28] A.M. Bolger, M. Lohse, B. Usadel, Trimmomatic: a flexible trimmer for Illumina sequence data, Bioinformatics 30 (15) (2014) 2114–2120.

[29] B. Li, C.N. Dewey, RSEM: accurate transcript quantification from RNA-Seq data with or without a reference genome, BMC Bioinformatics 12 (2011) 323.
[30] M.D. Robinson, D.J. McCarthy, G.K. Smyth, edgeR: a Bioconductor package for differential expression analysis of digital gene expression data, Bioinformatics 26 (1) (2010) 139–140.
[31] E. Eden, R. Navon, I. Steinfeld, D. Lipson, Z. Yakhini, GOrilla: a tool for discovery and visualization of enriched GO terms in ranked gene lists, BMC Bioinformatics 10 (1) (2009) 48.
[32] E. Eden, D. Lipson, S. Yogev, Z. Yakhini, Discovering motifs in ranked lists of DNA sequences, PLoS Comp. Biol. 3 (2007).
[33] W. Huang da, B.T. Sherman, R.A. Lempicki, Bioinformatics enrichment tools: paths toward the comprehensive functional analysis of large gene lists, Nucleic Acids Res. 37 (1) (2009) 1–13.
[34] D.W. Huang, B.T. Sherman, R.A. Lempicki, Systematic and integrative analysis of large gene lists using DAVID bioinformatics resources, Nat. Protocols 4 (1) (2008) 44–57.
[35] A. Psichas, G. Tolhurst, C.A. Brighton, F.M. Gribble, F. Reimann, Mixed primary cultures of murine small intestine intended for the study of gut hormone secretion and live cell imaging of enteroendocrine cells, J. Vis. Exp. 122 (2017).
[36] F. Reimann, A.M. Habib, G. Tolhurst, H.E. Parker, G.J. Rogers, F.M. Gribble, Glucose sensing in L cells: a primary cell study, Cell Metab. 8 (6) (2008) 532–539.
[37] E. Diakogiannaki, R. Pais, G. Tolhurst, H.E. Parker, J. Horscroft, B. Rauscher, T. Zietek, H. Daniel, F.M. Gribble, F. Reimann, Oligopeptides stimulate glucagon-like peptide-1 secretion in mice through proton-coupled uptake and the calcium-sensing receptor, Diabetologia 56 (12) (2013) 2688–2696.
[38] R. Pais, J. Rievaj, C. Meek, G. De Costa, S. Jayamaha, R.T. Alexander, F. Reimann, F. Gribble, Role of enteroendocrine L-cells in arginine vasopressin-mediated inhibition of colonic anion secretion, J. Physiol. 594 (17) (2016) 4865–4878.
[39] L.J. Lebrun, K. Lenaerts, D. Kiers, J.P. Pais de Barros, N. Le Guern, J. Plesnik, C. Thomas, T. Bourgeois, C.H.C. Dejong, M. Kox, I.H.R. Hundscheid, N.A. Khan, S. Mandard, V. Deckert, P. Pickkers, D.J. Drucker, L. Lagrost, J. Grober, Enteroendocrine L cells sense LPS after gut barrier injury to enhance GLP-1 secretion, Cell Rep. 21 (5) (2017) 1160–1168.
[40] G.W. Moran, C. O'Neill, J.T. McLaughlin, GLP-2 enhances barrier formation and attenuates TNFalpha-induced changes in a Caco-2 cell model of the intestinal barrier, Regul. Pept. 178 (1-3) (2012) 95–101.
[41] C.X. Dong, W. Zhao, C. Solomon, K.J. Rowland, C. Ackerley, S. Robine, M. Holzenberger, T. Gonska, P.L. Brubaker, The intestinal epithelial insulin-like growth factor-1 receptor links glucagon-like peptide-2 action to gut barrier function, Endocrinology 155 (2) (2014) 370–379.
[42] B. Yusta, L.L. Baggio, J. Koehler, D. Holland, X. Cao, L.J. Pinnell, K.C. Johnson-Henry, W. Yeung, M.G. Surette, K.W. Bang, P.M. Sherman, D.J. Drucker, GLP-1R agonists modulate enteric immune responses through the intestinal intraepithelial lymphocyte GLP-1R, Diabetes 64 (7) (2015) 2537–2549.
[43] J. Melissas, A. Leventi, I. Klinaki, K. Perisinakis, S. Koukouraki, E. de Bree, N. Karkavitsas, Alterations of global gastrointestinal motility after sleeve gastrectomy: a prospective study, Ann. Surg. 258 (6) (2013) 976–982.
[44] K. Suzuki, K. Iwasaki, Y. Murata, N. Harada, S. Yamane, A. Hamasaki, K. Shibue, E. Joo, A. Sankoda, Y. Fujiwara, Y. Hayashi, N. Inagaki, Distribution and hormonal characterization of primary murine L cells throughout the gastrointestinal tract, J. Diabetes Investig. (2017).
[45] H.J. Cho, S. Kosari, B. Hunne, B. Callaghan, L.R. Rivera, D.M. Bravo, J.B. Furness, Differences in hormone localisation patterns of K and L type enteroendocrine cells in the mouse and pig small intestine and colon, Cell Tissue Res. 359 (2) (2015) 693–698.
[46] K.V. Grunddal, C.F. Ratner, B. Svendsen, F. Sommer, M.S. Engelstoft, A.N. Madsen, J. Pedersen, M.K. Nøhr, K.L. Egerod, A.R. Nawrocki, T. Kowalski, A.D. Howard, S.S. Poulsen, S. Offermanns, F. Bäckhed, J.J. Holst, B. Holst, T.W. Schwartz, Neurotensin is coexpressed, coreleased, and acts together with GLP-1 and PYY in enteroendocrine control of metabolism, Endocrinology 157 (1) (2016) 176–194.
[47] K.L. Egerod, M.S. Engelstoft, K.V. Grunddal, M.K. Nøhr, A. Secher, I. Sakata, J. Pedersen, J.A. Windeløv, E.-M. Füchtbauer, J. Olsen, F. Sundler, J.P. Christensen, N. Wierup, J.V. Olsen, J.J. Holst, J.M. Zigman, S.S. Poulsen, T.W. Schwartz, A major lineage of enteroendocrine cells coexpress CCK, secretin, GIP, GLP-1, PYY, and Neurotensin but not somatostatin, Endocrinology 153 (12) (2012) 5782–5795.
[48] F.M. Gribble, F. Reimann, Enteroendocrine cells: chemosensors in the intestinal epithelium, Annu. Rev. Physiol. 78 (2016) 277–299.
[49] R.E. Kuhre, C.B. Christiansen, M.Y. Saltiel, N.J. Wewer Albrechtsen, J.J. Holst, On the relationship between glucose absorption and glucose-stimulated secretion of GLP-1, neurotensin, and PYY from different intestinal segments in the rat, Physiol. Rep. 5 (23) (2017).
[50] L.J. Billing, C.A. Smith, P. Larraufie, D.A. Goldspink, S. Galvin, R.G. Kay, J.D. Howe, R. Walker, M. Pruna, L. Glass, R. Pais, F.M. Gribble, F. Reimann, Co-storage and release of insulin-like peptide-5, glucagon-like peptide-1 and peptideYY from murine and human colonic enteroendocrine cells, Mol. Metab. 16 (2018) 65–75.
[51] A.J. Brown, S.M. Goldsworthy, A.A. Barnes, M.M. Eilert, L. Tcheang, D. Daniels, A.I. Muir, M.J. Wigglesworth, I. Kinghorn, N.J. Fraser, N.B. Pike, J.C. Strum, K.M. Steplewski, P.R. Murdock, J.C. Holder, F.H. Marshall, P.G. Szekeres, S. Wilson, D.M. Ignar, S.M. Foord, A. Wise, S.J. Dowell, The Orphan G protein-coupled receptors GPR41 and GPR43 are activated by propionate and other short chain carboxylic acids, J. Biol. Chem. 278 (13) (2003) 11312–11319.
[52] G. Tolhurst, H. Heffron, Y.S. Lam, H.E. Parker, A.M. Habib, E. Diakogiannaki, J. Cameron, J. Grosse, F. Reimann, F.M. Gribble, Short-chain fatty acids stimulate glucagon-like peptide-1 secretion via the G-protein-coupled receptor FFAR2, Diabetes 61 (2) (2012) 364–371.
[53] M.H.A. Muskiet, L. Tonneijck, M.M. Smits, M.J.B. van Baar, M.H.H. Kramer, E.J. Hoorn, J.A. Joles, D.H. van Raalte, GLP-1 and the kidney: from physiology to pharmacology and outcomes in diabetes, Nature reviews, Nephrology 13 (10) (2017) 605–628.
[54] Y.S. Lee, F. De Vadder, V. Tremaroli, A. Wichmann, G. Mithieux, F. Backhed, Insulin-like peptide 5 is a microbially regulated peptide that promotes hepatic glucose production, Mol. Metab. 5 (4) (2016) 263–270.
[55] J. Grosse, H. Heffron, K. Burling, M. Akhter Hossain, A.M. Habib, G.J. Rogers, P. Richards, R. Larder, D. Rimmington, A.A. Adriaenssens, L. Parton, J. Powell, M. Binda, W.H. Colledge, J. Doran, Y. Toyoda, J.D. Wade, S. Aparicio, M.B.L. Carlton, A.P. Coll, F. Reimann, S. O'Rahilly, F.M. Gribble, Insulin-like peptide 5 is an orexigenic gastrointestinal hormone, Proc. Natl. Acad. Sci. U. S. A. 111 (30) (2014) 11133–11138.
[56] L.L. Glass, F.J. Calero-Nieto, W. Jawaid, P. Larraufie, R.G. Kay, B. Gottgens, F. Reimann, F.M. Gribble, Single-cell RNA-sequencing reveals a distinct population of proglucagon-expressing cells specific to the mouse upper small intestine, Mol. Metab. 6 (10) (2017) 1296–1303.
[57] A.L. Haber, M. Biton, N. Rogel, R.H. Herbst, K. Shekhar, C. Smillie, G. Burgin, T.M. Delorey, M.R. Howitt, Y. Katz, I. Tirosh, S. Beyaz, D. Dionne, M. Zhang, R. Raychowdhury, W.S. Garrett, O. Rozenblatt-Rosen, H.N. Shi, O. Yilmaz, R.J. Xavier, A. Regev, A single-cell survey of the small intestinal epithelium, Nature 551 (7680) (2017) 333–339.
[58] J. Beumer, B. Artegiani, Y. Post, F. Reimann, F. Gribble, T.N. Nguyen, H. Zeng, M. Van den Born, J.H. Van Es, H. Clevers, Enteroendocrine cells switch hormone expression along the crypt-to-villus BMP signalling gradient, Nat. Cell Biol. 20 (8) (2018) 909–916.